Hispidulin exhibits potent anticancer activity *in vitro* and *in vivo* through activating ER stress in non-small-cell lung cancer cells

LI LV*, WENHUI ZHANG*, TINGTING LI, LIFENG JIANG, XINYAN LU and JIE LIN

Department of Medical Oncology, The Second Affiliated Hospital of Kunming Medical University, Kunming, Yunnan 650101, P.R. China

Received August 20, 2019; Accepted February 28, 2020

DOI: 10.3892/or.2020.7568

Abstract. Hispidulin is a medicinal natural compound isolated from *S. involucrata*, which exhibits potent anticancer properties. However, there are few reports on its effects on lung cancer cells. Therefore, the current study investigated the effects of hispidulin on cell viability and apoptosis in human non-small-cell lung cancer (NSCLC) cell lines NCI-H460 and A549 *in vitro* and *in vivo*. Methyl thiazolyl tetrazolium, colony formation assay, Hoechst 33342 staining, flow cytometry and western blotting were performed on Human NCI-H460 and A549 cells. A mouse xenograft model was also established using NCI-H460 cells. The results showed that the growth of NCI-H460 and A549 cells was inhibited, while apoptosis was promoted by hispidulin via increased generation of reactive oxygen species (ROS) in a dose-dependent manner. Furthermore, hispidulin triggered apoptosis in NSCLC cells through upregulating the expression of cleaved caspase-3 and cleaved poly [ADP-ribose] polymerase. All these effects were reversed upon pretreatment with glutathione, a selective ROS inhibitor. In addition, endoplasmic reticulum stress (ER stress) in NCI-H460 cells was activated by hispidulin. Pretreatment with tauroursodeoxycholic acid, a specific ER stress inhibitor, effectively reduced the cell apoptosis induced by hispidulin. In conclusion, hispidulin induces ROS-mediated apoptosis via activating the ER stress pathway. The current study provides theoretical basis for the antitumor effect of hispidulin in NSCLC.

Introduction

Lung cancer is the most common malignancy and one of the main causes of cancer-related mortality worldwide (1). It is estimated that 160,000 lung cancer-related deaths occurred in the United States in 2014, accounting for 20% of all cancer-related deaths (2). Non-small cell lung cancer (NSCLC) constitutes 80-85% of all lung cancer cases, with squamous cell carcinoma and adenocarcinoma as the two major subtypes (3). Though various treatment strategies including chemotherapy, pneumonectomy, radiation or combined modalities have been made available (4), the 5-year survival rate of patients with NSCLC remains unsatisfactory (5) and its molecular mechanism requires further investigation (6). Thus, it is essential to find new targets and therapies for NSCLC.

Natural products from medicinal plants have been studied widely to find important anticancer agents in the last decades (7). Hispidulin (4',5,7-trihydroxy-6-methoxyflavone; $C_{16}H_{12}O_6$; molecular weight, 300.3 g/mol) (Fig. 1A), a phenolic flavonoid isolated mainly from *S. involucrata*, was traditionally used in oriental medicine (8). Accumulated evidence has demonstrated that hispidulin has various effects, such as pro-oxidant, neuroprotective, anti-inflammatory, antiepileptic, antithrombotic, and antiosteoporotic activities (9-13). Furthermore, a number of *in vivo* and *in vitro* studies have shown that hispidulin has antitumor effects on diverse hematological and solid malignancies (14-17). The anticancer activities of hispidulin in acute myeloid leukemia, colorectal cancer, renal cell carcinoma, gallbladder cancer and hepatocellular carcinoma have also been confirmed (16-18). A previous study showed that hispidulin exerts proapoptotic and antiproliferative effects on HepG2 cells through reactive oxygen species (ROS)-induced endoplasmic reticulum stress (ER stress) (19). However, whether ER stress and apoptosis are related to the anticancer effect of hispidulin in NSCLC remains unclear.

The present study aimed to investigate the anticancer effects of hispidulin in NSCLC cells. Hispidulin induced NSCLC cell apoptosis in a time- and dose-dependent manner. Molecular mechanism studies have shown that apoptosis was regulated by ER stress activation induced by ROS. The results showed that the pro-apoptotic effect of hispidulin was associated with ROS-induced cell apoptosis through the activation of ER stress in NSCLC cells, which provided theoretical basis for the future research and development of clinical tumor-targeted drugs.

Correspondence to: Dr Jie Lin, Department of Medical Oncology, The Second Affiliated Hospital of Kunming Medical University, 374 Dianmian Avenue, Wuhua, Kunming, Yunnan 650101, P.R. China
E-mail: linjieshi@126.com

*Contributed equally

Key words: hispidulin, apoptosis, endoplasmic reticulum stress, reactive oxygen species, malignant tumor

Materials and methods

General reagents. Hispidulin (Shanghai Aladdin Bio-Chem Technology Co., Ltd.) was dissolved in 0.1% DMSO and 0.1% DMSO alone was used as the vehicle control. Tauroursodeoxycholic acid (TUDCA; Merck KGaA) was dissolved in saline. ROS probe 2',7'-dichlorodihydrofluorescein diacetate (DCFH-DA) was obtained from Beyotime Institute of Biotechnology and glutathione (GSH) was purchased from Sigma-Aldrich; Merck KGaA.

Cell culture and treatment. Human NSCLC cell lines NCI-H460 and A549 (Institute of Biochemistry and Cell Biology, Chinese Academy of Sciences) were cultured in RPMI-1640 media (Thermo Fisher Scientific, Inc.) with 10% FBS (Invitrogen; Thermo Fisher Scientific, Inc.), 100 U/ml penicillin and 100 μg/ml streptomycin. Cells were grown at 37˚C and 5% CO_2 (v/v) in a humidified cell incubator.

Determination of cell viability. Cell viability was determined by methyl thiazolyl tetrazolium (MTT). DMSO was used to dissolve the formazan product. The optical density of viable NCI-H460 and A549 cells was measured using a spectrophotometer at 450 nm (Tecan Group, Ltd.) following treatment with different concentrations of hispidulin (0, 4, 8, 15, 30 and 60 μM) for 24 or 48 h. Cell viability assays were performed in triplicate.

Colony formation assay. NCI-H460 and A549 cells (1,000 cells/well) were cultured in a six-well plate. The cultures were maintained for 12 h upon 5 and 10 μM hispidulin treatment, and cells were grown for 8-11 days with fresh medium (RPMI-1640 with 10% FBS) at 37˚C in a humidified 5% CO_2 atmosphere. The cells were subsequently fixed with 4% paraformaldehyde for 15 min at room temperature, stained with crystal violet for 30 min, and photographed using a digital camera (Nikon DXM-1200; Nikon Corporation).

Flow cytometry analysis. FITC Annexin V/PI apoptosis kit (BD Pharmingen; BD Biosciences) was used to determine cell apoptosis. Cells were pretreated with 2.5 mM TUDCA prior to treatment with 30 μM hispidulin for 24 h. The NCI-H460 and A549 cells were collected, washed, and resuspended in 195 μl Annexin V-FITC-binding buffer. Following this, cells were incubated with Annexin V-FITC and PI (5 μl each) for 15 min at 4˚C. The cells were analyzed by Accuri C6 plus flow cytometry (BD Biosciences). The flow cytometry data were quantified using Flow Jo 7.6.1 software (Tree Star, Ashland, Inc.).

Hoechst 33342 staining. Cell nuclear staining was performed using a Hoechst 33342 Staining kit (Beyotime Institute of Biotechnology). The NCI-H460 and A549 cells were incubated in Hoechst 33342 (2 μg/ml) for 30 min at 37˚C 24 h post hispidulin treatment. Then, the stained cells were examined by using a fluorescence microscope.

Measurement of ROS generation. NCI-H460 cells were seeded in six-well plates and incubated for 24 h. After pretreatment with 5 mM GSH for 1 h and treatment with the 15 and 30 μM hispidulin for 3 h, the cells were incubated with 10 μM DCFH-DA for 20 min at 37˚C in the dark. The cells were subsequently washed twice with PBS and the levels of intracellular ROS were analyzed immediately using a fluorescence microscope (Nikon Corporation). The fluorescence intensity measurements were performed using ImageJ (National Institutes of Health).

Western blotting. NCI-H460 cells were cultured with hispidulin (15 or 30 μM) for 4 or 24 h and collected. Cells were pretreated with 2.5 mM TUDCA prior to treatment with 30 μM hispidulin for 24 h. Proteins were isolated from the hispidulin-treated or control DMSO-treated cells and the protein concentrations were determined using the bicinchoninic acid protein assay kit (cat. no. P0010; Beyotime Institute of Biotechnology). Total proteins (~50 μg/lane) were subjected to 10% SDS-PAGE and transferred to a PVDF membrane which was blocked with 5% (w/v) low-fat milk for 1 h at room temperature. The membrane was subsequently incubated with the following primary antibodies, cleaved-poly [ADP-ribose] polymerase (PARP; cat. no. sc-56196; 1:200), caspase3 (cat. no. sc-56053; 1:1,000) and GAPDH (cat. no. sc-32233; 1:1,000) purchased from Santa Cruz Biotechnology, Inc. and ATF4 (cat. no. 11815; 1:1,000), phospho (p)-eukaryotic translation initiation factor 2 subunit α (EIF2α; cat. no. 3398; Ser51; 1:1,000), EIF2α (cat. no. 5324; 1:1,000), C/EBP-homologous protein (CHOP; cat. no. 2895; 1:1,000), cleaved-caspase3 (cat. no. 9664; 1:1,000) purchased from Cell Signaling Technology, Inc. overnight at 4˚C. Horseradish peroxidase (HRP)-conjugated secondary antibodies (cat. nos. sc-2317 and sc-2318; 1:2,000) purchased from Santa Cruz Biotechnology Inc. were incubated with membrane for 1.5 h at room temperature. The blot signal was detected using a chemiluminescent substrate (KPL, Inc.). BandScan software (Glyko Biomedical, Ltd.) was used for densitometry. All assays were performed in triplicate.

NCI-H460 xenograft tumor growth in nude mice. A total of 18 male athymic BALB/c mice (8 weeks old; 18-19 g) were housed at a constant room temperature with a 12/12-h light/dark cycle and fed a standard rodent diet under standard pathogen-free conditions. All animal experiments were approved by the Institutional Animal Care and Use Committee of the Second Affiliated Hospital of Kunming Medical University. NCI-H460 cells ($1x10^6$) were subcutaneously injected into the left dorsal flanks of the BALB/c mice. A total of 15 days after cell injection, mice were divided randomly into three groups (6 mice/group): Vehicle group (0.9% sodium chloride with 1% DMSO), low dose group (20 mg/kg hispidulin) and high dose group (40 mg/kg hispidulin) once every 2 days for 20 days. Mice body weight and tumor volumes were measured every 3 days for 21 days. All mice were euthanized with CO_2 and serum samples were aliquoted into sterile tubes, centrifuged at 1,100 x g for 10 min at room temperature for subsequent analysis. The activities of aspartate transaminase (AST) and alanine transaminase (ALT) were analyzed by using a VetScan analyzer (Abaxis, Inc.). Assay kits of AST and ALT were purchased from Abcam (cat. nos. ab105134 and ab105135). The harvested heart, liver and kidney tissues of mice were used for hematoxylin and eosin (H&E) staining. Immunohistochemical (IHC) staining were performed on NCI-H460 cell-derived

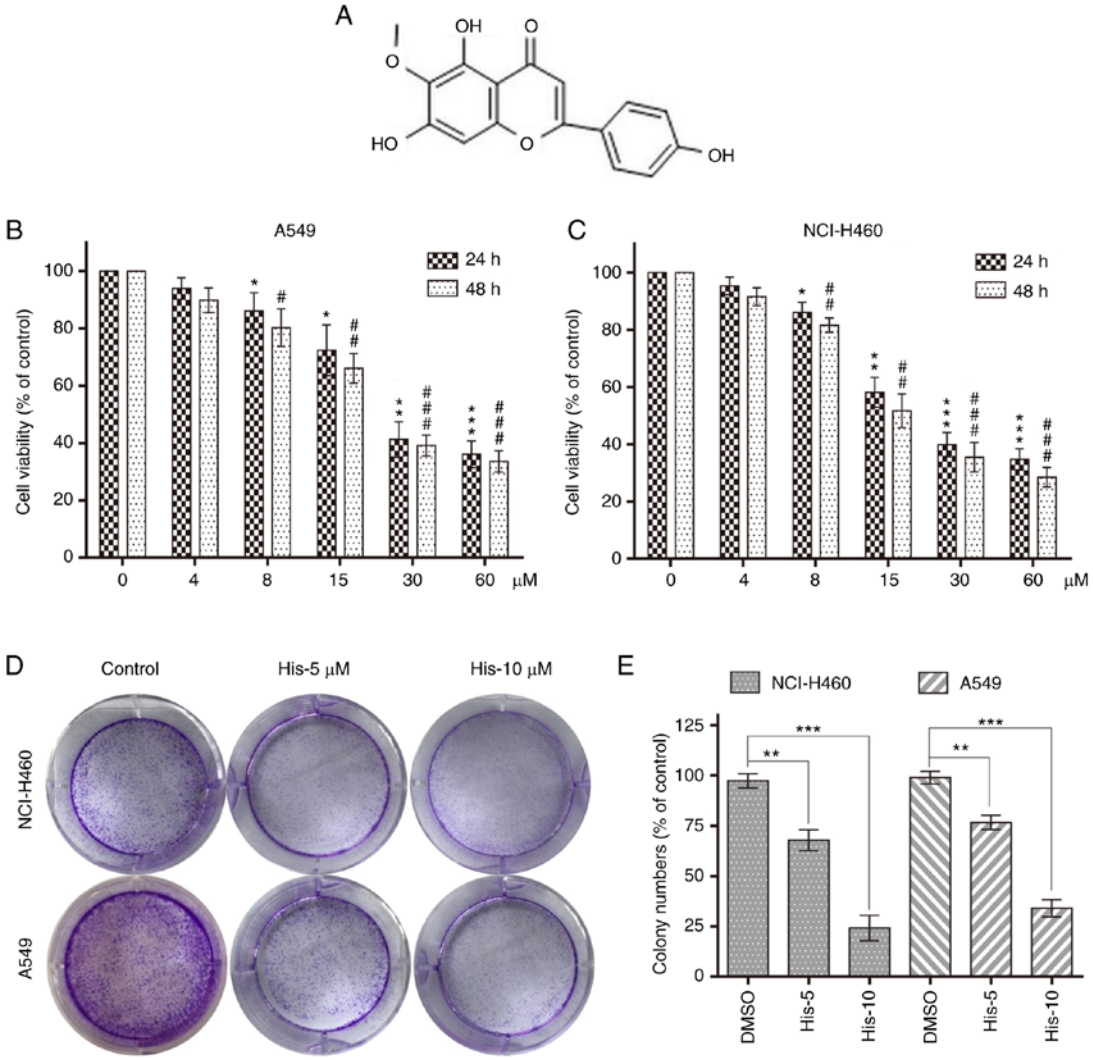

Figure 1. Hispidulin inhibits cell viability in human NSCLC cells. (A) Chemical structure of hispidulin. Cell viability was analyzed using MTT assay in (B) A549 and (C) NCI-H460 cells treated with His (4, 8, 15, 30 and 60 μM) for 24 or 48 h. *P<0.05, **P<0.01, ***P<0.001 compared to DMSO control at 24 h. $^{\#}$P<0.05, $^{\#\#}$P<0.01, $^{\#\#\#}$P<0.001 compared to DMSO control at 48 h. (D) Effect of different His concentrations (5 and 10 μM) on human NSCLC colony formation. NCI-H460 and A549 cells were incubated with His for 12 h and allowed to grow for 8-11 days. Colonies were stained by crystal violet dye. (E) The colony formation ability of each group was shown in bar chart. **P<0.01, ***P<0.001 as indicated. All images shown are representative of three independent experiments with similar results. Data are shown as mean ± SEM (n=3). His, hispidulin; NSCLC, non-small-cell lung cancer; His-5, 5 μM hispidulin; His-10, 10 μM hispidulin.

xenograft tumors as previously described (20). The following primary antibodies were used for IHC: Proliferation marker protein Ki-67 (1:50; cat. no sc-7846; Santa Cruz Biotechnology, Inc.), cleaved-caspase 3 (1:100; cat. no. 9664; Cell Signaling Technology, Inc.) and p-EIF2α (1:1,000; cat. no. 3398; Cell Signaling Technology, Inc). HRP-conjugated secondary antibodies (cat. nos. sc-2317 and sc-2031) were purchased from Santa Cruz Biotechnology, Inc. Caspase-3 activity in tumor lysates was determined using a caspase-3 activity kit (Beyotime Institute of Biotechnology) according to the kit instructions.

Statistical analysis. Data are presented as the mean ± SEM from three separate experiments. Statistical comparisons between cells were performed by using one-way ANOVA and Dunnett's t test when comparing more than two groups of data with control group, two-way ANOVA, non-parametric Kruskal-Wallis test, followed by Dunn's post hoc test when comparing multiple independent groups and one-way repeated measures ANOVA followed by Dunnett's post hoc test when comparing tumor volume and animal body weight. Experimental data were analyzed by using GraphPad Prism software (version 8.0; GraphPad Software, Inc.). P<0.05 was considered to indicate a statistically significant difference.

Results

Hispidulin effectively suppresses the cell survival in human NSCLC cells. To explore the effect of hispidulin treatment on cell viability, human NSCLC cells (NCI-H460 and A549) were treated with various concentrations of hispidulin (0, 4, 8, 15, 30 and 60 μM/l) for 24 and 48 h. The MTT assay results showed that hispidulin markedly decreased the viability of A549 and NCI-H460 cell lines in a time- and concentration-dependent manner (Fig. 1B and C). Additionally, 5 and 10 μM hispidulin was used to treat NCI-H460 and A549 cells for 12 h followed

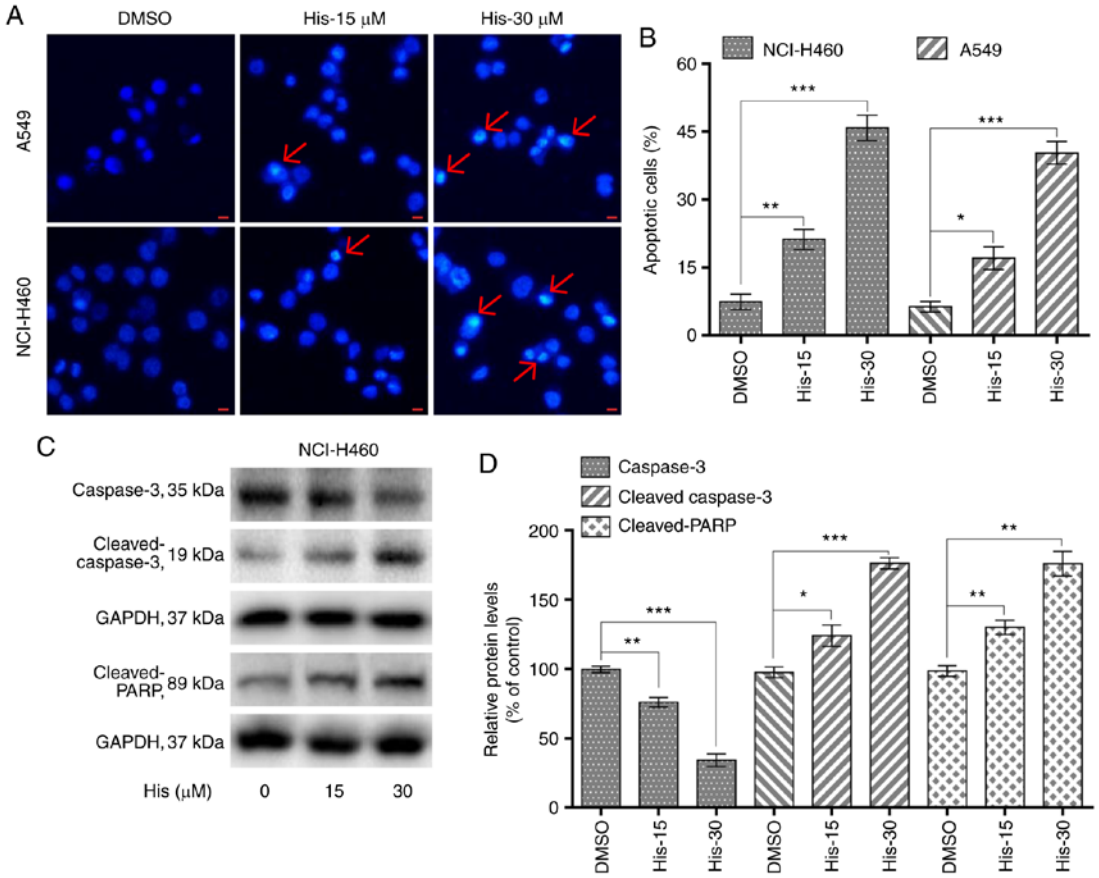

Figure 2. Hispidulin promotes cell apoptosis in a dose-dependent manner in human non-small-cell lung cancer cells. (A) Hoechst 33342 staining analysis of the apoptotic cell population after NCI-H460 and A549 cells were exposed to 15 and 30 μM His for 24 h. The apoptotic cells were observed under a fluorescence microscope. Red arrows indicate apoptotic cells (scale bar=10 μm). (B) NCI-H460 and A549 cells were treated with 15 and 30 μM His for 24 h, then flow cytometry was used to quantify the percentage of apoptotic cells through Annexin-V/PI staining. (C) Expression levels of apoptosis-related proteins, including cleaved PARP, cleaved caspase 3 and caspase 3 were determined by western blotting after treatment with 15 or 30 μM His for 24 h in NCI-H460 cells. GAPDH was used as internal control. (D) Quantification of western blotting. All images shown are representative of three independent experiments with similar results. Data are shown as the mean ± SEM (n=3). *P<0.05, **P<0.01 and ***P<0.001 vs. the DMSO group. PARP, poly [ADP-ribose] polymerase; His, hispidulin; His-15, 15 μM hispidulin; His-30, 30 μM hispidulin.

by a culture in a new medium for 8-11 days. Colony formation results showed that the colony formation ability was inhibited following treatment with 5 and 10 μM hispidulin compared with the control group (Fig. 1D and E). These results revealed that hispidulin inhibited the viability of NCI-H460 and A549 cells in a time and dose-dependent manner.

Hispidulin induces apoptosis in human NSCLC cells in a dose-dependent manner. To explore whether hispidulin induced apoptosis in NCI-H460 and A549 cells, flow cytometric analysis and Hoechst 33342 staining was performed. Hoechst staining results showed that 15 and 30 μM hispidulin treatment for 24 h lead to cell apoptosis in a dose-dependent manner in both cell lines (Fig. 2A). Flow cytometry results indicated that treatment with hispidulin (15 and 30 μM) for 24 h lead to a significant increase in the percentage of apoptotic cells (Annexin V-FITC^{+}/PI^{-} and Annexin V-FITC^{+}/PI^{+} rates). The proapoptotic effect induced by hispidulin occurred in a concentration-dependent manner (Figs. 2B and S1). Additionally, NCI-H460 cells were treated with 15 and 30 μM hispidulin for 24 h and western blotting results showed that the expression levels of caspase 3 were markedly downregulated after exposure to the increasing concentrations of hispidulin compared with the DMSO group. However, the expression levels of proteolytic cleaved forms of caspase-3 as well as cleaved PARP were found to be upregulated (Fig. 2C and D), which revealed that hispidulin treatment could induce caspase-3 activation and apoptosis in NCI-H460 cells.

Hispidulin induces ROS-mediated apoptosis in human NSCLC cells. To investigate the role of ROS in hispidulin-induced apoptosis, the ROS level was measured in NCI-H460 cells treated with various concentrations of hispidulin for 3 h. The results showed that the ROS level was significantly increased by hispidulin in a concentration-dependent manner (Fig. 3A and B). However, pre-treatment of NCI-H460 cells with 5 mM ROS scavenger GSH showed a significantly decreased level of ROS compared with the hispidulin-treated cells (Fig. 3C and D). Further western blotting results indicated that GSH pre-treatment attenuated hispidulin-induced expression of apoptosis-related proteins in NCI-H460 cells (Fig. 3E and F). The same results were observed using the Annexin V/PI staining assay (Fig. 3G and H). These results demonstrated that ROS generation was significantly involved in hispidulin-induced apoptosis.

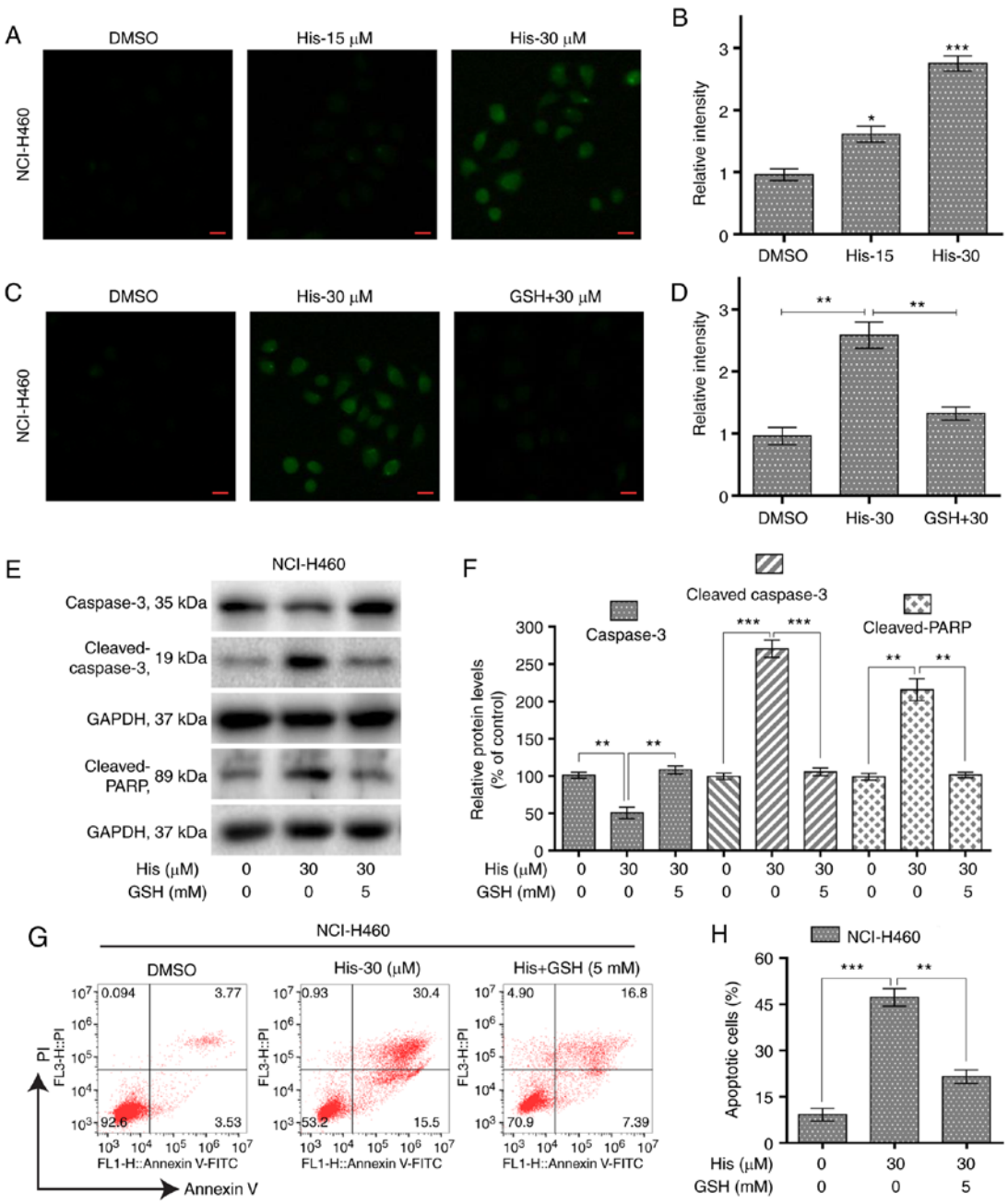

Figure 3. Hispidulin induces ROS-dependent apoptosis in human non-small-cell lung cancer cells. (A) Intracellular ROS generation induced by treatment with 15 and 30 μM His for 3 h was measured in NCI-H460 cells by staining with 10 μM DCFH-DA. The ROS levels were observed under a fluorescence microscope (scale bar=20 μm). (B) Quantification of ROS level data following treatment with His. *P<0.05 and ***P<0.001 vs. the DMSO group. (C) NCI-H460 cells were pre-incubated with or without 5 mM GSH for 1 h before exposure to His at 30 μM for 3 h. Intracellular ROS generation was measured by fluorescence microscopy (scale bar=20 μm). (D) Quantification of ROS level data following treatment with GSH and His. (E) Expression levels of apoptosis-related proteins cleaved PARP, cleaved caspase 3 and caspase 3 were determined by western blotting after treatment with His (30 μM) or His (30 μM) + GSH (5 mM) for 24 h in NCI-H460 cells. GAPDH was used as internal control. (F) Quantification of western blotting data. (G) The percentage of apoptotic cells was quantified by Annexin-V/PI staining after treatment with His (30 μM), His (30 μM) + GSH (5 mM) for 24 h. (H) Quantitative analysis of flow cytometry results. All images shown are representative of three independent experiments with similar results. Data are shown as mean ± SEM (n=3). **P<0.01 and ***P<0.001 as indicated. PARP, poly [ADP-ribose] polymerase; GSH, glutathione; His, hispidulin; His-15, 15 μM hispidulin; His-30, 30 μM hispidulin; GSH + 30, 5 mM glutathione + 30 μM hispidulin.

Hispidulin causes ER stress activation and cell apoptosis in NSCLC cells. To explore the relationship between ER stress and cancer cell apoptosis, the expression levels of ER stress-related proteins including p-eIF2α and cyclic AMP-dependent transcription factor ATF4 were detected in NCI-H460 cells treated with hispidulin. Western blot analysis results revealed that the expression of p-eIF2α and ATF4 were increased upon 4-h hispidulin treatment in a dose-dependent manner (Figs. 4A and B and S2). CHOP is an important factor mediating ER stress-induced apoptosis (21). The current study found that 10-h hispidulin treatment lead to a significant increase in the protein expression level of CHOP (Fig. 4A and B). Then the role of ROS in hispidulin-induced ER stress progress was evaluated. The expression of p-eif2α, ATF4 and CHOP was

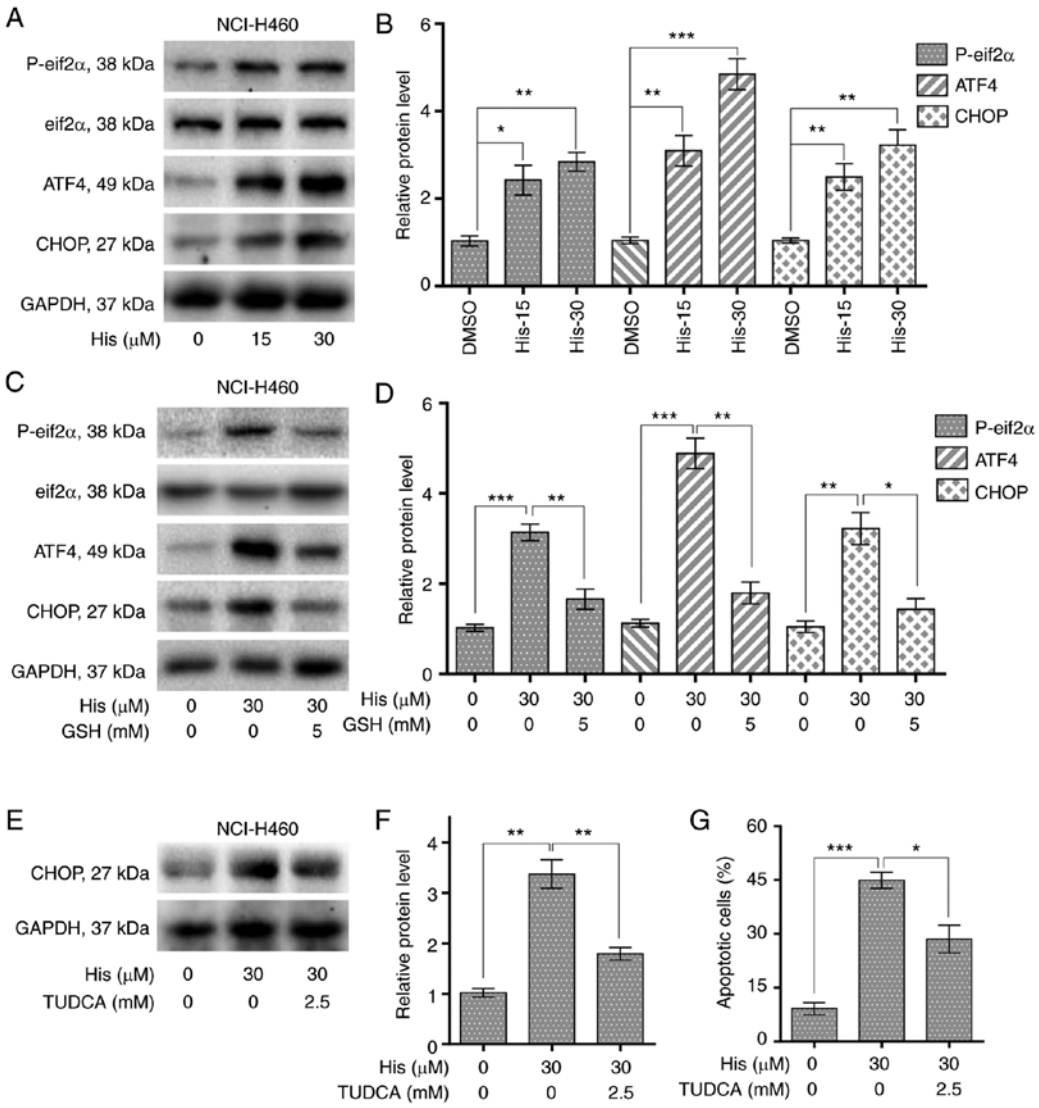

Figure 4. Hispidulin induces apoptosis through ROS-dependent ER stress pathway in human NSCLC cells. (A) Protein expression of ER stress pathway-associated proteins, p-eIF2α, eIF2α, ATF4 and CHOP in human NSCLC cells. NCI-H460 cells were exposed to 15 and 30 μM His for 4 h for p-eIF2α, eIF2α and ATF4 or 10 h for CHOP. (B) Quantification of western blotting results flowing treatment with His. (C) Protein expression of ERs pathway-associated proteins, p-eIF2α, eIF2α, ATF4 and CHOP in human NSCLC cells exposed to 30 μM His and 5 mM GSH. (D) Quantification of western blotting results flowing treatment with His and GSH. (E) Effect of TUDCA pretreatment on His-induced CHOP protein expression in NCI-H460 cells. TUDCA was used at 2.5 mM for 1 h before exposure to 30 μM His. (F) Quantification of CHOP protein expression levels. (G) Effect of TUDCA on His-induced apoptosis in NCI-H460 cells was determined by Annexin V/PI staining. TUDCA was used at 2.5 mM for 1 h before exposure to His. All images shown are representative of three independent experiments with similar results. Data are presented as the mean ± SEM, n=3. *P<0.05, **P<0.01 and ***P<0.001 as indicated. GSH, glutathione; His, hispidulin; TUDCA, tauroursodeoxycholic acid; ATF4, cyclic AMP-dependent transcription factor ATF4; p-, phosphorylated; eIF2α, eukaryotic translation initiation factor 2 subunit α; CHOP, C/EBP-homologous protein; NSCLC, non-small-cell lung cancer.

significantly decreased upon 5 mM GSH pre-treatment for 1 h compared with hispidulin treatment alone in NCI-H460 cells (Figs. 4C and D and S2). TUDCA, a chemical chaperone frequently used for block the ER stress process (22), was used to investigate whether ER stress was involved in the anticancer effect of hispidulin. Pre-treatment with TUDCA (2.5 mM) for 1 h in NCI-H460 and A549 cells effectively reversed the increase in CHOP protein expression levels induced by treatment with hispidulin for 10 h (Figs. 4E and F and S3A and B). Besides, Pre-treatment of NCI-H460 or A549 cells with TUDCA significantly decreased apoptosis rate induced by Hispidulin treatment for 24 h (Figs. 4G and S3C and D). All these findings demonstrate that hispidulin-induced cell apoptosis may be mediated through activation of the ER stress pathway.

Hispidulin suppresses NSCLC xenograft tumor growth in nude mice. The *in vivo* effect of hispidulin was assessed using an NSCLC xenograft mouse model. NCI-H460 cells were implanted in BALB/c mice and then the mice were injected with different doses of hispidulin (20 and 40 mg/kg) or vehicle control. Hispidulin attenuated the xenograft tumor growth compared with vehicle group at both doses 21 days after the first treatment (Fig. 5A). However, there were no significant differences in the body weights of the mice in different treatment groups (Fig. 5B). Moreover, the side effects of hispidulin were evaluated using normal hepatocytes of tumor-bearing mice. The effects on serum makers of liver function including ALT and AST were tested immediately at the end of the treatment. There was no significant

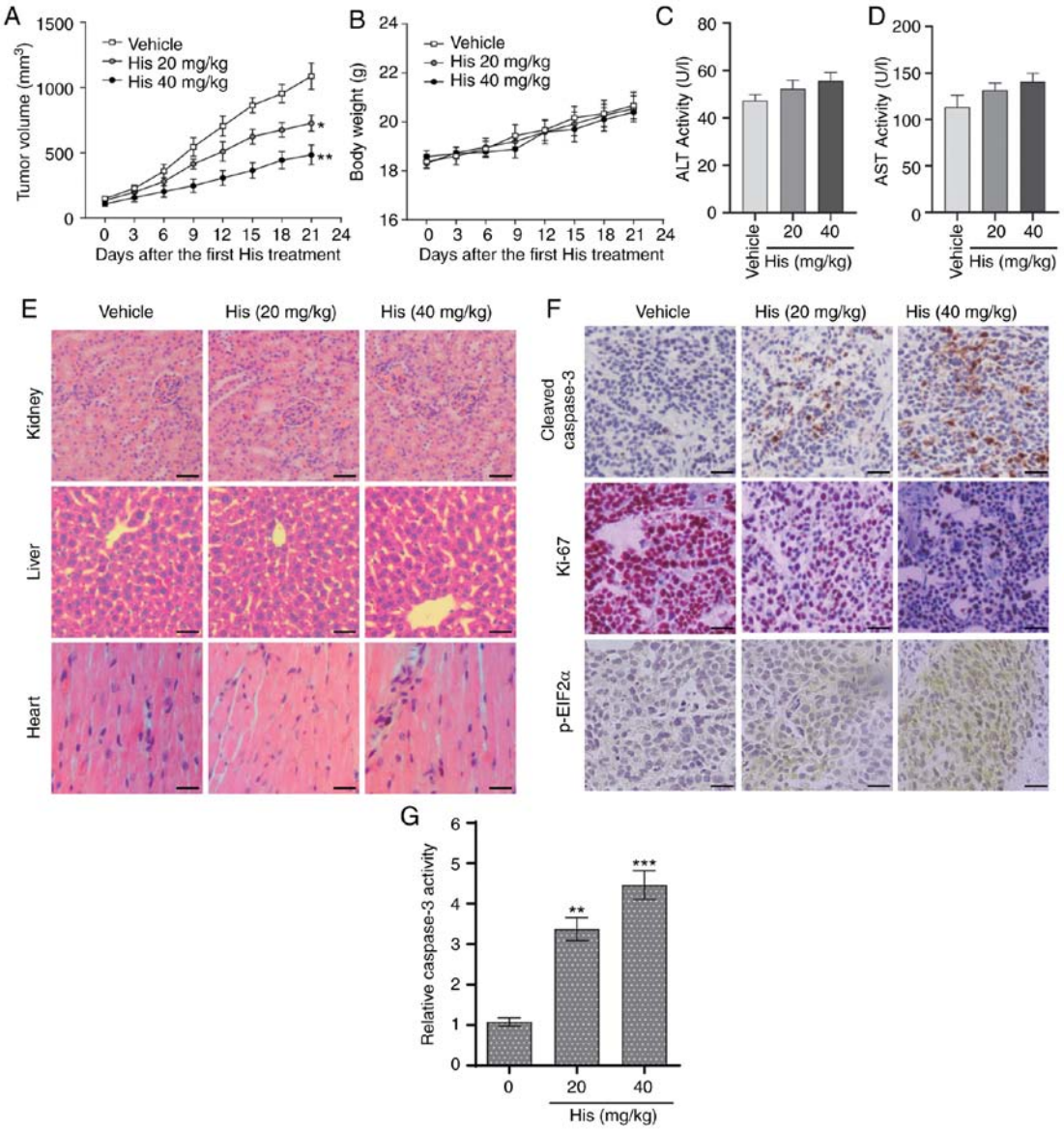

Figure 5. Hispidulin suppresses the growth of NSCLC xenografts in nude mice. (A) Vehicle or 20 and 40 mg/kg His were intraperitoneally injected into tumor-bearing nude mice for 3 weeks, and tumor growth was monitored every 3 days. (B) Measurement of the body weight every 3 days in a NSCLC xenograft mice model after treatment with different dosages of His or vehicle. Serum samples were collected from tumor-bearing mice and serum activities of (C) ALT and (D) AST were detected. Values were normalized to those from the vehicle control group. (E) Kidneys, livers and heart tissues were sectioned at 5 μm and the slides were stained with hematoxylin and eosin. All images were obtained at x20 magnification. Hispidulin administration did not cause histological abnormalities in kidneys, livers and hearts (scale bar=50 μm). (F) Immunohistochemical staining was performed on the cryostat sections (5-μm thick) of NSCLC xenograft tumors to detect the expression of cleaved caspase-3, p-eIF2α and Ki-67 after treatment with hispidulin (scale bar=50 μm). (G) At the end of the study, tumor tissue lysates were prepared and subjected to caspase-3 activity assay. Data are presented as the mean ± SEM, n=6. *P<0.05, **P<0.01 and ***P<0.001 vs. the vehicle group. His, hispidulin; ALT, alanine transaminase; AST, aspartate transaminase; Ki-67, proliferation marker protein Ki-67; p-eIF2α, phosphorylated eukaryotic translation initiation factor 2 subunit α; NSCLC, non-small-cell lung cancer.

difference in these indices between the vehicle group and hispidulin-treated groups (Fig. 5C and D). Furthermore, H&E staining showed that hispidulin treatment did not induce marked histological changes compared with the vehicle group (Fig. 5E). IHC staining was used to assess the protein expression of representative tumor progression (Ki-67), ER stress (p-eIF2α) or apoptosis marker (cleaved caspase-3) markers in the xenograft tumors which were harvested from the three groups. The results revealed that Ki-67 expression was decreased in the His-treated groups compared with the vehicle group, while the cleaved caspase-3 and p-eIF2α expression levels were increased (Fig. 5F). Furthermore, hispidulin effectively induced cell apoptosis *in vivo,* as verified by caspase-3 activity assay (Fig. 5G). These results suggested that hispidulin induced NSCLC xenograft tumor growth inhibition as well as apoptosis *in vivo.*

Discussion

The current study investigated the anticancer effect of hispidulin in human NSCLC cells. Our results revealed that hispidulin inhibited proliferation and induced apoptosis in NSCLC cells. In addition, hispidulin induced ROS-dependent apoptosis in human NSCLC cells and caused ER stress

activation. The hispidulin-induced cell apoptosis effect was mediated through the activation of the ER stress pathway.

Hispidulin is a natural bioactive flavone with pharmacological effects. Previous studies have demonstrated that hispidulin inhibited gastric cancer cell growth in a time- and concentration-dependent manner by inducing G_1/S phase arrest and apoptosis (18,23,24). Furthermore, hispidulin inhibited human pancreatic tumor growth *in vivo* in xenograft model mice. Vascular endothelial growth factor-induced cell invasion, migration, and capillary-like structure formation were also inhibited by hispidulin (25). The effect of hispidulin on the liver system has also been reported (15). However, the molecular mechanisms of anticancer effect induced by hispidulin in NSCLC cells remain unclear.

The elevated generation of ROS triggers caspase-related pathways resulting in apoptosis (26-28). Therefore, the current study detected the levels of ROS in NSCLC cells treated with different concentrations of hispidulin and pretreated with GSH, a selective ROS inhibitor. The results suggested that ROS was markedly involved in hispidulin-induced apoptosis.

ER stress is a regulator of different pathologies and an important mechanism of cancer cell death due to therapeutic drugs (29,30). In certain cases, oxidative stress and ER stress occur simultaneously, and are closely linked to signaling events (31,32). The proline-rich receptor-like protein kinase (PERK) signaling is mediated through phosphorylation of eIF2α and PERK phosphorylates multiple substrates to protect cells from oxidative stress (33,34). IRE1α-dependent mitogen-activated protein kinase activation can activate CHOP to contribute to ROS generation (35). Further, ROS can also regulate ER stress-induced apoptotic responses through the ER-calcium signaling (36). The levels of ER stress-related proteins, such as ATF4 and p-eIF2α in hispidulin-treated NCI-H460 cells were detected in the current study and hispidulin treatment increased the levels of p-eIF2α and ATF4 in a dose-dependent manner. CHOP is involved in repressing transcription of the anti-apoptotic BCL2 protein, leading to enhanced oxidant injury and apoptosis. Previous studies have shown that the antitumor capacity of numerous small molecule anti-tumor compounds that activate the ER stress pathway is significantly reduced after silencing CHOP protein (37,38).

Based on the results of the current *in vitro* study, an NCI-H460 xenograft mouse model was used to test the *in vivo* therapeutic effects of hispidulin. Previous research revealed that injection of isoliensinine significantly suppressed the Huh-7 xenograft tumors (39). In the current study, hispidulin markedly inhibited the tumor growth at doses of 20 and 40 mg/kg. The mouse body weight was not significantly affected by hispidulin in HCC xenograft mouse models (15). Consistent with this finding, the current study found that the body weight of NCI-H460 xenograft mouse models changed slightly at both doses and was not significantly different compared with vehicle control. In a previous study, isoliensinine induced cell apoptosis in xenograft HCC tissues *in vivo*, as demonstrated by a caspase-3 activity assay (40). Similarly, as demonstrated in the current study, hispidulin had the capacity to induce cell apoptosis *in vivo*.

In conclusion, hispidulin lead to cell apoptosis through ROS-mediated ER stress in NSCLC cells. This study began to elucidate the underlying mechanism of hispidulin in NSCLC, and indicated that targeting ER stress and ROS may be an effective step in the development of anti-NSCLC drugs.

Acknowledgements

Not applicable.

Funding

This study was supported by grants from the Research of Yunnan Science and Technology Planning Project [grant no. 2017FE468 (-201)], the China Health Promotion Foundation Anti-angiogenesis Research Project (grant no. JJKXG20170503), the National Natural Science Foundation of China (grant no. 81960423) and the Second Affiliated Hospital of Kunming Medical University Program (grant no. 2019YK001).

Availability of data and materials

The datasets used and/or analyzed during the present study are available from the corresponding author on reasonable request.

Authors' contributions

JL conceived and designed that study. LL and WZ acquired, analyzed and interpreted the data. TL, LJ and XL participated in the study design, data collection and revision process. All authors read and approved the final manuscript.

Ethics approval and consent to participate

All animal experiments were approved by the Institutional Animal Care and Use Committee of the Second Affiliated Hospital of Kunming Medical University.

Patient consent for publication

Not applicable.

Competing interests

The authors declare that they have no competing interests.

References

1. Siegel R, Naishadham D and Jemal A: Cancer statistics, 2012. CA Cancer J Clin 62: 10-29, 2012.
2. Yang F, Sui X, Chen X, Zhang L, Wang X, Wang S and Wang J: Sublobar resection versus lobectomy in surgical treatment of elderly patients with early-stage non-small cell lung cancer (STEPS): Study protocol for a randomized controlled trial. Trials 17: 191, 2016.
3. Shtivelman E, Hensing T, Simon GR, Dennis PA, Otterson GA, Bueno R and Salgia R: Molecular pathways and therapeutic targets in lung cancer. Oncotarget 5: 1392-1433, 2014.
4. Li S, Fan J, Liu J, Zhou J, Ren Y, Shen C and Che G: Neoadjuvant therapy and risk of bronchopleural fistula after lung cancer surgery: A systematic meta-analysis of 14 912 patients. Jpn J Clin Oncol 46: 534-546, 2016.
5. Socinski MA, Stinchcombe TE, Moore DT, Gettinger SN, Decker RH, Petty WJ, Blackstock AW, Schwartz G, Lankford S, Khandani A and Morris DE: Incorporating bevacizumab and erlotinib in the combined-modality treatment of stage III non-small-cell lung cancer: Results of a phase I/II trial. J Clin Oncol 30: 3953-3959, 2012.

6. Wagner KW, Alam H, Dhar SS, Giri U, Li N, Wei Y, Giri D, Cascone T, Kim JH, Ye Y, *et al*: KDM2A promotes lung tumorigenesis by epigenetically enhancing ERK1/2 signaling. J Clin Invest 123: 5231-5246, 2013.
7. Bishayee A and Sethi G: Bioactive natural products in cancer prevention and therapy: Progress and promise. Sem Cancer Biol 40: 1-3, 2016.
8. Xu YJ, Zhao DX, Fu CX, Cheng LQ, Wang NF, Han LJ and Ma FS: Determination of flavonoid compounds from Saussurea involucrata by liquid chromatography electrospray ionisation mass spectrometry. Nat Prod Res 23: 1689-1698, 2009.
9. Yin Y, Gong FY, Wu XX, Sun Y, Li YH, Chen T and Xu Q: Anti-Inflammatory and immunosuppressive effect of flavones isolated from artemisia vestita. J Ethnopharmacol 120: 1-6, 2008.
10. Zhou R, Wang Z and Ma C: Hispidulin exerts anti-osteoporotic activity in ovariectomized mice via activating AMPK signaling pathway. Cell Biochem Biophys 69: 311-317, 2014.
11. Yang JM, Hung CM, Fu CN, Lee JC, Huang CH, Yang MH, Lin CL, Kao JY and Way TD: Hispidulin sensitizes human ovarian cancer cells to TRAIL-Induced apoptosis by AMPK activation leading to Mcl-1 block in translation. J Agric Food Chem 58: 10020-10026, 2010.
12. Xie J, Gao H, Peng J, Han Y, Chen X, Jiang Q and Wang C: Hispidulin prevents hypoxia-induced epithelial-mesenchymal transition in human colon carcinoma cells. Am J Cancer Res 5: 1047-1061, 2015.
13. Lee-Hilz YY, Boerboom AM, Westphal AH, Berkel WJ, Aarts JM and Rietjens IM: Pro-Oxidant activity of flavonoids induces EpRE-Mediated gene expression. Chem Res Toxicol 19: 1499-1505, 2006.
14. Wang YG, Liu W, He X and Fei Z: Hispidulin enhances the anti-tumor effects of temozolomide in glioblastoma by activating AMPK. Cell Biochem Biophys 71: 701-706, 2015.
15. Han M, Gao H, Xie J, Yuan YP, Yuan Q, Gao MQ, Liu KL, Chen XH, Han YT and Han ZW: Hispidulin induces ER stress-mediated apoptosis in human hepatocellular carcinoma cells in vitro and in vivo by activating AMPK signaling pathway. Acta Pharmacol Sin 40: 666-676, 2019.
16. Liu K, Gao H, Wang Q, Wang L, Zhang B, Han Z, Chen X, Han M and Gao M: Hispidulin suppresses cell growth and metastasis by targeting PIM1 through JAK2/STAT3 signaling in colorectal cancer. Cancer Sci 109: 1369-1381, 2018.
17. Gao MQ, Gao H, Han M, Liu KL, Peng JJ and Han YT: Hispidulin suppresses tumor growth and metastasis in renal cell carcinoma by modulating ceramide-sphingosine 1-phosphate rheostat. Am J Cancer Res 7: 1501-1514, 2017.
18. Gao H, Gao MQ, Peng JJ, Han M, Liu KL and Han YT: Hispidulin mediates apoptosis in human renal cell carcinoma by inducing ceramide accumulation. Acta Pharmacol Sin 38: 1618-1631, 2017.
19. Scoparo C, Valdameri G, Worfel P, Guterres FA, Martinez GR, Winnischofer SM, Di Pietro A and Rocha ME: Dual properties of hispidulin: Antiproliferative effects on HepG2 cancer cells and selective inhibition of ABCG2 transport activity. Mol Cell Biochem 409: 123-133, 2015.
20. Han Y, Yang X, Zhao N, Peng J, Gao H and Qiu X: Alpinumisoflavone induces apoptosis in esophageal squamous cell carcinoma by modulating miR-370/PIM1 signaling. Am J Cancer Res 6: 2755-2771, 2016.
21. Zinszner H, Kuroda M, Wang XZ, Batchvarova N, Ron D, Lightfoot RT, Remotti H and Stevens JL: CHOP is implicated in programmed cell death in response to impaired function of the endoplasmic reticulum. Genes Dev 12: 982-995, 1998.
22. Launay N, Ruiz M, Grau L, Ortega FJ, Ilieva EV, Martínez JJ, Galea E, Ferrer I, Knecht E, Pujol A and Fourcade S: Tauroursodeoxycholic bile acid arrests axonal degeneration by inhibiting the unfolded protein response in X-linked adrenoleukodystrophy. Acta Neuropathol 133: 283-301, 2017.
23. Yu CY, Su KY, Lee PL, Jhan JY, Tsao PH, Chan DC and Chen YL: Potential therapeutic role of hispidulin in gastric cancer through induction of apoptosis via NAG-1 signaling. Evid Based Complement Alternat Med 2013: 518301, 2013.
24. Lin YC, Hung CM, Tsai JC, Lee JC, Chen YL, Wei CW, Kao JY and Way TD: Hispidulin potently inhibits human glioblastoma multiforme cells through activation of AMP-activated protein kinase (AMPK). J Agric Food Chem 58: 9511-9517, 2010.
25. He L, Wu Y, Lin L, Wang J, Wu Y, Chen Y, Yi Z, Liu M and Pang X: Hispidulin, a small flavonoid molecule, suppresses the angiogenesis and growth of human pancreatic cancer by targeting vascular endothelial growth factor receptor 2-mediated PI3K/Akt/mTOR signaling pathway. Cancer Sci 102: 219-225, 2011.
26. Lu Z, Zhang G, Zhang Y, Hua P, Fang M, Wu M and Liu T: Isoalantolactone induces apoptosis through reactive oxygen species-dependent upregulation of death receptor 5 in human esophageal cancer cells. Toxicol Appl Pharmacol 352: 46-58, 2018.
27. Jin C, Zhang G, Zhang Y, Hua P, Zhang X, Song G, Sun M, Li X, Tong T and Li B: Isoalantolactone induces intrinsic apoptosis through p53 signaling pathway in human lung squamous carcinoma cells. PLoS One 12: e0181731, 2017.
28. Brentnall M, Rodriguez-Menocal L, De Guevara RL, Cepero E and Boise LH: Caspase-9, caspase-3 and caspase-7 have distinct roles during intrinsic apoptosis. BMC Cell Biol 14: 32, 2013.
29. Huang P, Zhang YH, Zheng XW, Liu YJ, Zhang H, Fang L, Zhang YW, Yang C, Islam K, Wang C and Naranmandura H: Phenylarsine oxide (PAO) induces apoptosis in HepG2 cells via ROS-mediated mitochondria and ER-stress dependent signaling pathways. Metallomics 9: 1756-1764, 2017.
30. Yang J, Wei J, Wu Y, Wang Z, Guo Y, Lee P and Li X: Metformin induces ER stress-dependent apoptosis through miR-708-5p/NNAT pathway in prostate cancer. Oncogensis 193: e158, 2015.
31. Maryam A, Mehmood T, Yan Q, Li Y, Khan M and Ma T: Proscillaridin A promotes oxidative stress and ER stress, inhibits STAT3 activation, and induces apoptosis in A549 lung adenocarcinoma cells. Oxid Med Cell Longev 11: 3853409, 2018.
32. Zhang L, Sang BK, Luitel K and Shay JW: Cholesterol depletion by TASIN-1 induces apoptotic cell death through the ER Stress/ROS/JNK signaling in colon cancer cells. Mol Cancer Ther 17: 943-951, 2018.
33. Ron D: Translational control in the endoplasmic reticulum stress response. J Clin Invest 110: 1383-1388, 2002.
34. Scheuner D, Song B, Mcewen E, Liu C, Laybutt R, Gillespie P, Saunders T, Bonner-Weir S and Kaufman RJ: Translational control is required for the unfolded protein response and in vivo glucose. Mol Cell 7: 1165-1176, 2001.
35. Harding HP, Zhang Y, Zeng H, Novoa I, Lu PD, Calfon M, Sadri N, Yun C, Popko B, Paules R, *et al*: An integrated stress response regulates amino acid metabolism and resistance to oxidative stress. Mol Cell 11: 619-633, 2003.
36. Malhotra JD and Kaufman RJ: Endoplasmic reticulum stress and oxidative stress: A vicious cycle or a double-edged sword? Antioxid Redox Signal 9: 2277-2294, 2007.
37. Lee DH, Jung Jung Y, Koh D, Lim Y, Lee YH and Shin SY: A synthetic chalcone, 2'-hydroxy-2,3,5'-trimethoxychalcone triggers unfolded protein response-mediated apoptosis in breast cancer cells. Cancer Lett 372: 1-9, 2016.
38. Prasad S, Yadav VR, Ravindran J and Aggarwal BB: ROS and CHOP are critical for dibenzylideneacetone to sensitize tumor cells to TRAIL through induction of death receptors and down-regulation of cell survival proteins. Cancer Res 71: 538-549, 2011.
39. Shu G, Yue L, Zhao W, Xu C, Yang J, Wang S and Yang X: Isoliensinine, a bioactive alkaloid derived from embryos of nelumbo nucifera, induces hepatocellular carcinoma cell apoptosis through suppression of NF-κB signaling. J Agric Food Chem 63: 8793-8803, 2015.
40. Zhang W, Liu S, Liu K, Ji B, Wang Y and Liu Y: Knockout of ADAM10 enhances sorafenib antitumor activity of hepatocellular carcinoma in vitro and in vivo. Oncol Rep 32: 1913-1922, 2014.